

Fundamental solutions of a conservation law without convexity^{*}

YONG-JUNG KIM, YOUNGSOO HA^{**}

Abstract

In this paper we construct fundamental solutions of a scalar conservation law in one space dimension. These source-type solutions are well known for a convex flux case and our focus is on a non-convex case which may have a finite number of inflection points. Signed fundamental solutions are constructed first and then under the assumption of a positive flux two parameters family of fundamental solutions are constructed. This process is a natural generalization of N-waves. New N-waves constructed here consist of a series of increasing rarefaction waves and increasing shocks and then another series of decreasing rarefaction waves and decreasing shocks. This fundamental solution indicates why the famous one sided Oleinik estimate fails for a non-convex case and how it should be corrected. N-waves are also computed using the WENO and central type numerical schemes, which show the structure of the N-wave constructed in this paper.

1. Introduction

Fundamental or source-type solutions such as the Gaussian for the heat equation and Barenblatt-type solutions for nonlinear diffusion equations have played a key role in the theoretical development of such differential equations. In many cases the fundamental solution reflects the intrinsic property of the equation such as the similarity structure. Therefore, the structure of the fundamental solution helps us to understand the evolution of general solutions. The asymptotics usually means a study of the process

^{*} This work was supported by the Korea Science and Engineering Foundation(KOSEF) grant funded by the Korea government(MOST) (No.R01-2007-000-11307-0).

^{**} Corresponding Author

how does a general solution turn into a fundamental solution like shape (see, e.g., [2, 10, 12]). A fundamental solution is also used as a tool to derive various estimates needed in the analysis. The heat equation is an extreme case that a general solution itself is given exactly from the fundamental solution which is a convolution with the initial value. Even for a nonlinear case the source-type solution may help to construct a general solution (see [9]).

In many cases fundamental solutions are explicit. For example, if the diffusion is given by a power law, the similarity structure of the problem enables us to find a fundamental solution explicitly, which is called the Barenblatt solution. A fundamental or a source-type solution to a conservation law is a solution to

$$u_t + f(u)_x = 0, \quad \lim_{t \rightarrow 0} u(x, t) = M\delta(x), \quad x \in \mathbf{R}, t > 0, \quad (1)$$

where the initial value is in the distribution sense and $M \in \mathbf{R}$ is the total mass. We take a smooth flux $f \in C^1$ and may assume

$$f(0) = f'(0) = 0 \quad (2)$$

without loss of generality. The uniqueness of the problem has been shown by Liu and Pierre [15] when the flux is odd. For a positive flux the uniqueness is obtained among signed solutions and, if sign-changing solutions are included, the source-type solution is not unique in general.

The fundamental solution of a diffusion equation is an integrable signed function which is unique for a given total mass $M \in \mathbf{R}$. For a conservation law with a convex flux, the fundamental solution is not unique and given explicitly as a member of two parameter family of functions which are called N-waves. However, for a non-convex flux case, the fundamental solution is barely understood.

The theory of nonlinear convex conservation laws was highlighted because it explains the shock wave phenomenon excellently which was not possible with linear models. There has been intensive studies on the convex case and it is now well understood (see [3, 13, 14, 18]). However, the convex case is still in a stage between a local and a global behavior of the conservation laws and one should go non-convex case to see the real global structure (see, e.g., [16, 20, 21] for non-convex flux cases). Then there are a lot more interesting features such as contact discontinuity and emerging centered and non-centered rarefaction waves (see, e.g., [4, 19]). Even though this non-convex case has been studied for a long time (see, e.g., [1]), we are still far from an understanding as satisfactory as the convex flux case and that is partly because we do not have fundamental solutions.

This paper is about the construction of fundamental solutions of conservation laws without the convexity assumption. We first construct a signed source-type solution under the following hypothesis:

$$f = f(u) \text{ has only a finite number of inflection points,} \quad (H1) \\ f(u)/|u| \rightarrow \infty \quad \text{as} \quad |u| \rightarrow \infty,$$

where the divergence in the second assumption is monotone for $|u| > C$ for some $C > 0$ large. These hypotheses are technical. The first one on the finite number of inflection points is to construct convex and concave envelopes by connect humps with a finite number of lines. If one consider a bounded solution, the value of the flux at $|u|$ near infinity does not make any difference and therefore one may always assume the second one.

For the case $M > 0$ we construct a positive solution which is denoted by $N_{0,M}(x, t)$. If $M < 0$, the corresponding solution $N_{|M|,0}(x, t)$ is negative. (Notice that we use positive indices.) We call them signed N-waves which are one parameter family of solutions. The two parameter family of N-waves are then constructed by

$$N_{p,q}(x, t) = N_{p,0}(x, t) + N_{0,q}(x, t), \quad (3)$$

where the positive indices satisfy

$$M = -p + q, \quad p, q \geq 0. \quad (4)$$

Since the problem is not linear, the N-wave $N_{p,q}(x, t)$ is not a solution of (1) in general. However, under the second hypothesis

$$f(u) \geq 0 \quad \text{for } u \in \mathbf{R}, \quad (H2)$$

we will see that $N_{p,q}(x, t)$ is a solution. The initial value of the problem is clearly satisfied since

$$\lim_{t \rightarrow 0} N_{p,q}(x, t) (= -p\delta(x-) + q\delta(x+)) = M\delta(x). \quad (5)$$

in the distribution sense. From the uniqueness theory [15] there is no more source-type solution other than N-waves in (3) under Hypotheses (H1, 2). However, the uniqueness of the signed N-waves under Hypothesis (H1) only is not clear.

Closing the introduction consider one indication of the fundamental solution introduced here. For the convex case the Oleinik-type one sided entropy estimate $f'(u)_x \leq 1/t$ actually reflects the structure of the N-wave of the convex case and gives the uniqueness of solutions. However this kind of estimate does not hold for a non-convex case and, furthermore, this estimate does not give the uniqueness (see [6, 7]). Therefore, one should find a different estimate and the new one should reflect the structure of fundamental solutions for the non-convex case.

The rest of the paper consists as followings. In Section 2 we briefly give some preliminaries about admissible weak solutions and explicit N-waves for the Burgers and a general convex cases. In Section 3 convex-concave envelopes of a non-convex flux are considered. Using these envelopes we construct fundamental solutions in Section 4 and show that they are admissible weak solutions. Some of the basic structures are also introduced in the section. In Section 5 several numerical examples for source-type solutions are given and compared with the ones constructed in this paper.

2. Preliminary: N-waves for convex cases

The solution of the equation (1) is defined in a weak sense that satisfies

$$\int \int (u\phi_t + f(u)\phi_x) dx dt + \int u_0(x)\phi(x, 0) dx = 0 \quad (6)$$

for any test function $\phi \in C_0^\infty(\mathbf{R} \times [0, \infty))$. If a weak solution has a discontinuity at $x = x(t)$, then it should satisfy the Rankine-Hugoniot jump condition

$$x'(t) = \frac{f(u_r) - f(u_l)}{u_r - u_l}, \quad u_l = \lim_{y \uparrow x} u(y, t), \quad u_r = \lim_{y \downarrow x} u(y, t). \quad (7)$$

On the other hand a weak solution is not unique and hence one should consider a physically meaningful one. We always consider solutions that satisfy the Oleinik entropy condition, i.e., a weak solution $u(x, t)$ satisfies

$$l(u) \leq f(u) \text{ for all } u_l < u < u_r, \text{ and } l(u) \geq f(u) \text{ for all } u_r < u < u_l, \quad (8)$$

where $l(u)$ is the linear function connecting two states u_r and u_l , i.e.,

$$l(u) = \frac{f(u_l) - f(u_r)}{u_l - u_r}(u - u_l) + f(u_l). \quad (9)$$

A discontinuity that satisfies the admissibility condition is called a shock. Then an entropy solution exists and is unique for a bounded measurable initial value and the solution of (1) always means this weak solution that satisfies this entropy condition. For the well-posedness of the entropy solutions we refer to [1, 18]. In summary the admissible solution satisfies the equation in a classical sense in smooth regions and discontinuity satisfies the Rankine-Hugoniot and Oleinik conditions. Furthermore if a function satisfies the equation in classical sense in the smooth regions and the Rankine-Hugoniot and Oleinik conditions, then it is the admissible solution.

The N-waves for the Burgers equation are well known and one may find them from various text books. The construction of N-waves for a general flux without the convexity assumption is more complicated than the convex case. However the basic structure of the convex case also plays the key role. To compare the similarity and the difference more clearly we start with simpler cases.

2.1. N-waves for the Burgers equation

For the Burgers case, the equation is written as

$$u_t + uu_x = 0, \quad \lim_{t \rightarrow 0} u(x, t) = M\delta(x), \quad x \in \mathbf{R}, \quad t > 0. \quad (10)$$

Then the N-wave is given explicitly by

$$N_{p,q}(x, t) = \begin{cases} x/t, & -\sqrt{2pt} < x < \sqrt{2qt}, \\ 0, & \text{otherwise.} \end{cases} \quad (11)$$

One can easily check that this N-wave satisfies the Burgers equations in the smooth regions by simple substitutions. The Oleinik and the Rankine-Hugoniot conditions are satisfied along the possible two jump discontinuity curves $x = -\sqrt{2pt}$ and $x = \sqrt{2qt}$. Hence this N-wave is an entropy solution of the problem (10). One can also easily check the initial condition.

2.2. N-waves for a convex case

Now consider a convex flux case

$$u_t + h(u)_x = 0, \quad h''(u) > 0, \quad \lim_{t \rightarrow 0} u(x, t) = M\delta(x), \quad x \in \mathbf{R}, \quad t > 0. \quad (12)$$

In this case the derivative of the convex flux function h' is invertible and the rarefaction profile ' $g(x)$ ' is defined as the inverse of $h'(x)$, i.e.,

$$g = (h')^{-1} \quad \text{or} \quad h'(g(x)) = x, \quad x \in \mathbf{R}. \quad (13)$$

Then the N-wave is explicitly given by

$$N_{p,q}(x, t) = \begin{cases} g(x/t), & -a_p(t) < x < b_q(t), \\ 0, & \text{otherwise,} \end{cases} \quad (14)$$

where $a_p(t)$ and $b_q(t) \geq 0$ satisfy

$$p = - \int_{-a_p(t)}^0 g(y/t) dy, \quad q = \int_0^{b_q(t)} g(y/t) dy. \quad (15)$$

The relations in (15) are to satisfy the condition (5). One can similarly check that this N-wave satisfies (12) in the smooth regions by simple substitutions and the Oleinik and Rankine-Hugoniot conditions are satisfied along the possible two jump discontinuity curves $x = -a_p(t)$ and $x = b_q(t)$ since the flux is convex and the limits satisfy $u_l > u_r$ at the jumps.

For the Burgers case one can easily see that the rarefaction profile is $g(x) = x$ and hence $g(x/t) = x/t$. For this case the equation (15) is easily solved and given by $a_p(t) = \sqrt{2tp}$ and $b_q(t) = \sqrt{2tq}$. In Figure 1 examples of N-waves are plotted for the Burgers case and the case with $f(u) = |u|^3/3$. We displayed the positive part only for the sake of saving space.

3. Convex and concave envelopes for a non-convex flux

Now we return to the original problem (1) under the hypothesis (H1).

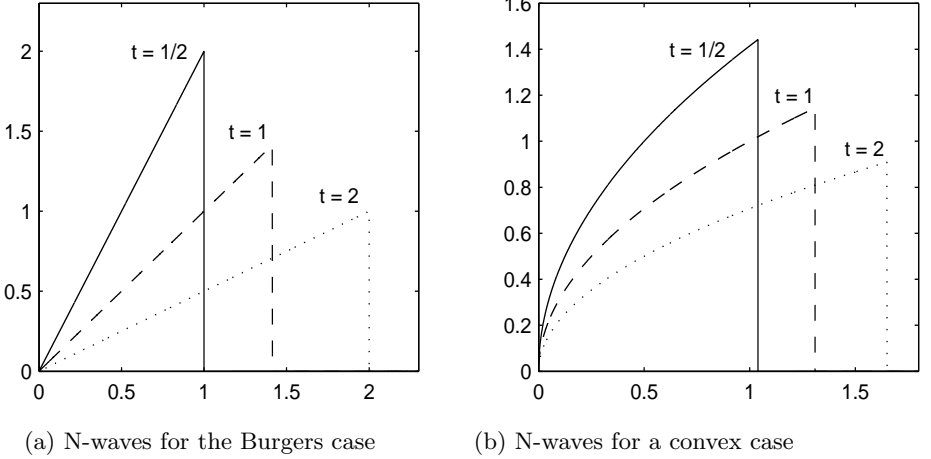


Fig. 1. Graphs of N-wave $N_{0,1}(x, t)$ are given at three instances $t = 0.5, 1$ and 2 . For the other convex case (b) the flux function is given by $f(u) = |u|^3/3$.

3.1. Convex envelope and the increasing side of an N-wave

The first step to construct an N-wave is to find the lower convex envelope of the given flux. For a given interval $u \in (\underline{u}, \bar{u})$, it is defined as

$$h(u; \underline{u}, \bar{u}) := \sup_{\eta \in A(\underline{u}, \bar{u})} \eta(u), \quad (16)$$

where

$$A(\underline{u}, \bar{u}) := \{\eta \in C^2(\mathbf{R}) : \eta''(u) \geq 0, \eta(u) \leq f(u) \text{ for } \underline{u} < u < \bar{u}\}. \quad (17)$$

Since there are only finite number of inflection points, the convex envelope $h(u; \underline{u}, \bar{u})$ is obtained by simply connecting the humps of the graph of the flux and the end points \underline{u}, \bar{u} with tangent lines. For the case $\underline{u} = -\infty$ and $\bar{u} = \infty$, we simply write it as $h(u)$ (see Figure 2).

The convex envelope $h(u)$ is continuously differentiable and is linear on intervals on which $f(u) \neq h(u)$. There exist strictly increasing sequences $b_i, c_i, i = 1, 2, \dots, n$, such that

$$h'(u) = \begin{cases} c_i, & b_{2i-1} < u < b_{2i}, \\ f'(u), & \text{otherwise.} \end{cases} \quad (18)$$

It is clear that h' is not invertible. However, the function $g(x)$ can be given by the second relation in (13) which is

$$g(0) = 0, \quad h'(g(x)) = x, \quad x \in \mathbf{R}. \quad (19)$$

Then $g(x)$ is piecewise continuous with jump discontinuities at c_i 's from $\lim_{x \uparrow c_i} g(x) = b_{2i-1}$ to $\lim_{x \downarrow c_i} g(x) = b_{2i}$ (see Figure 3(b)). In other words

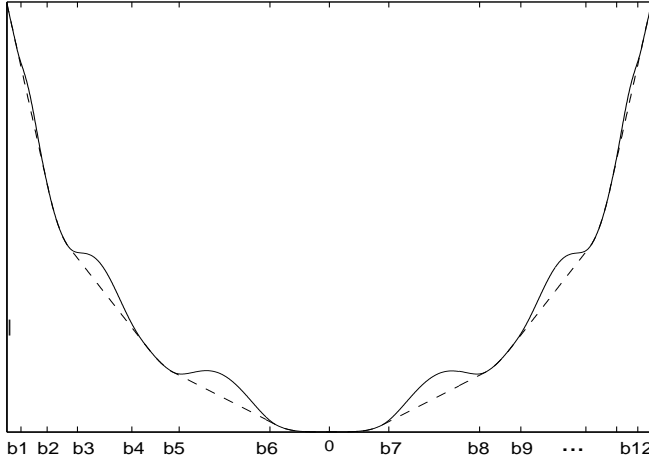


Fig. 2. An example of a non-convex flux $f(u)$ satisfying hypotheses in (H1-2) is given in a solid line. Its convex envelope $h(u)$, dashed line, is linear on intervals (b_{2i-1}, b_{2i}) , $i = 1, \dots, 6$, and agrees with the flux $f(u)$ on the intervals (b_{2i}, b_{2i+1}) , $i = 0, \dots, 6$, where $b_0 = \underline{u}$ and $b_{13} = \bar{u}$.

the function $g(x)$ consists of shocks and rarefaction waves. This profile gives the increasing side of the N-wave.

Now define N-wave like functions as

$$\tilde{N}_{p,q}(x, t) = \begin{cases} g(x/t), & -\tilde{a}_p(t) < x < \tilde{b}_q(t), \\ 0, & \text{otherwise,} \end{cases} \quad (20)$$

where $p, q \geq 0$ and $\tilde{a}_p(t), \tilde{b}_q(t) \geq 0$ satisfy

$$p = - \int_{-\tilde{a}_p(t)}^0 g(y/t) dy, \quad q = \int_0^{\tilde{b}_q(t)} g(y/t) dy. \quad (21)$$

(see Figure 4) One can easily check that this function satisfies the equation in (1) in the smooth regions and the relation (5). At the increasing jumps the Oleinik entropy condition (8) is satisfied since h is the convex envelope of f . The Rankine-Hugoniot jump condition is also satisfied. Therefore, $\tilde{N}_{p,q}(x, t)$ is a source-type solution of (1) as long as the jumps at $x = -\tilde{a}_p(t)$ and $x = \tilde{b}_q(t)$ satisfy the Oleinik entropy condition (8). However, it is not the case and they are not a solution in general.

Remark 1. It is natural to ask when $\tilde{N}_{p,q}(x, t)$ in (20) becomes a source-type solution. One can easily see that if the graph of $f(u)$ is star-shaped with respect to the origin, the discontinuity at $x = \tilde{b}_q(t)$ is admissible and hence it is a solution. Under (H2) the flux is convex for small $|u| \ll 1$. Therefore, there exists $T > 0$ such that $\tilde{N}_{p,q}(x, t)$ satisfies the convection equation

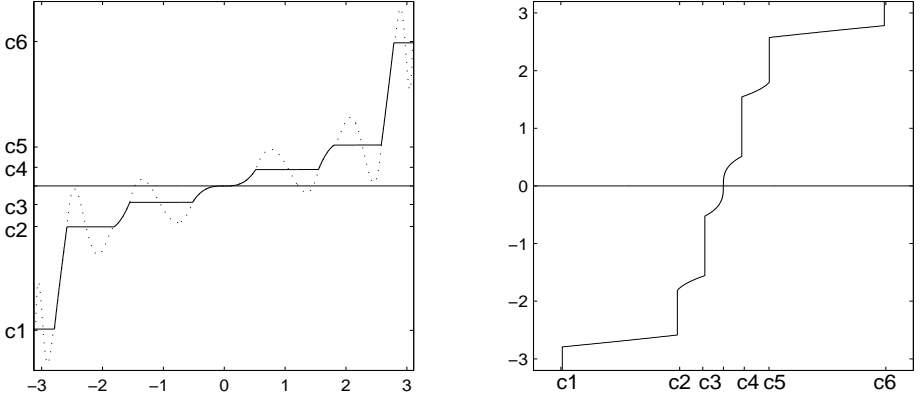
(a) Comparison: $f'(u)$ and $h'(u)$ (b) Rarefaction profile $g(x)$

Fig. 3. (a) The graphs of $f'(u)$ and $h'(u)$ for the flux in Figure 2. (b) The rarefaction profile $g(x)$ satisfies the inverse relation (19) and has an increasing jump at c_i that connects b_{2i-1} and b_{2i} .

for $t > T$. From the Figure 4 the waves seem to satisfy the equation for $t > 20$. The second hypothesis in (H1) implies that there exists \bar{u} such that the jump that connects the zero to $u > \bar{u}$ satisfies the entropy condition. Therefore, $\tilde{N}_{p,q}(x, t)$ is a solution for $t \ll 1$ small.

Remark 2. If the flux f is strictly convex, the the rarefaction profile $g(x)$ is continuous. If not, $g(x)$ may have discontinuities. We call a continuous part a rarefaction wave and a discontinuous part a shock. However, the jumps in the profile also move with continuous part without changing its shape as in $g(x/t)$ until it meets a decreasing side. Notice that this shock is a different from the one of the convex case in Figure 1.

Remark 3. The profile $g(x)$ provides the crucial information about the source-type solution when Hypothesis (H2) holds and the over all structure of the flux looks like the one in Figure 2. For the general case with Hypothesis (H1) only, the convex envelope plays the same role as the concave envelope in the following section.

3.2. Concave envelope and decreasing side of an N-wave

The second step to construct an N-wave is to find the upper concave envelope of the flux. For a given interval $u \in (\underline{u}, \bar{u})$ it is given by

$$k(u; \underline{u}, \bar{u}) := \inf_{\eta \in B(\underline{u}, \bar{u})} \eta(u), \quad (22)$$

where

$$B(\underline{u}, \bar{u}) := \{\eta \in C^2(\mathbf{R}) : \eta''(u) \leq 0, \eta(u) \geq f(u) \text{ for } \underline{u} < u < \bar{u}\}. \quad (23)$$

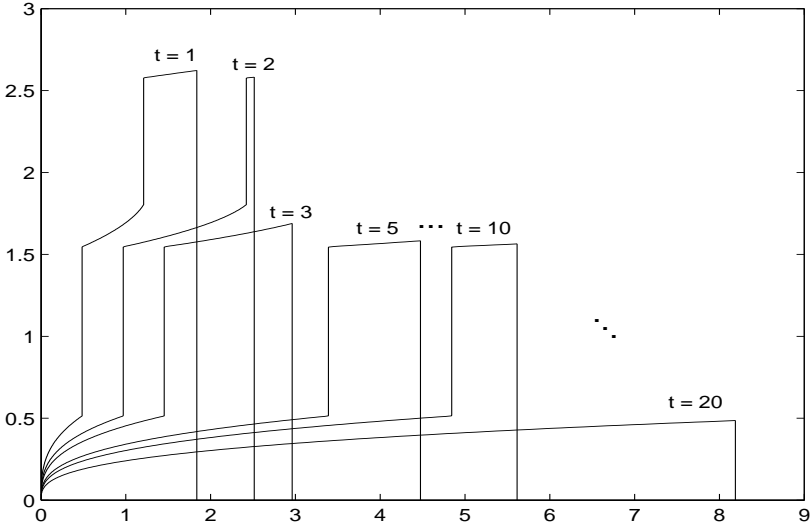


Fig. 4. Graphs of N-wave like functions ‘ $\tilde{N}_{0,3}(x, t)$ ’ in (20) are given at several instances $t = 1, 2, 3, 5, 10$ and 20 . One can find the rarefaction profile of Figure 3 (b) from them. After $t = 20$ only the profile in the interval $b_6 < u < b_7$ left and increasing discontinuities are all gone.

Since there is only finite number of inflection points, the concave envelope $k(u; \underline{u}, \bar{u})$ is similarly obtained by connecting the humps of the graph of $y = f(u)$ and the end points from the above with tangent lines (see Figure 5). The concave envelope is the dual concept of the convex envelope and decides the shape of the decreasing side of an N-wave. If one assumes $f'(u) < 0$ for all $u \neq 0$ instead of (H2), then one should have constructed $\tilde{N}_{p,q}$ in (20) employing the concave envelope instead of the convex one.

Remark 4. Consider a Riemann problem with an initial value

$$u_0(x) = \begin{cases} u_l, & x < 0, \\ u_r, & x > 0. \end{cases}$$

Then, the solution $u(x, t)$ is simply given by inverse relations

$$\begin{aligned} th'(u(x, t); u_l, u_r) &= x, & \text{if } u_l < u_r, \\ tk'(u(x, t); u_r, u_l) &= x, & \text{if } u_l > u_r. \end{aligned}$$

This simplicity is due to that the convex hull does not vary since the maximum and the minimum values are fixed. However, for the fundamental solution case, the maximum decreases and hence the convex hull varies in time. To count this behavior the left hand side should be understood as an integral in time variable and, for the non-convex case, it is written as in (29) and (33).

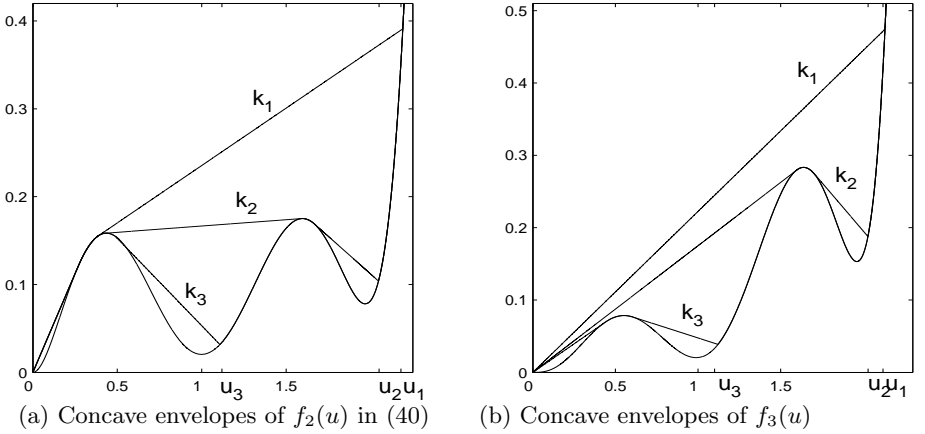


Fig. 5. Concave envelopes $k_i := k(u; 0, u_i)$ (22). They give decreasing profiles of an N-wave. A linear part indicates that there is a shock connecting two end values. A tangent part means that there is a rarefaction wave that connects two end values. Figures show variety of possibilities depending on the height of an N-wave.

We consider several obvious relations between concave and convex envelopes in the following lemma.

Lemma 1. *The convex and concave envelopes are ordered as*

$$h(u; u_1, u_2) \leq k(u; u_3, u_4), \quad u \in (u_1, u_2) \cap (u_3, u_4). \quad (24)$$

If $(u_1, u_2) \subset (u_3, u_4)$, then

$$k(u; u_1, u_2) \leq k(u; u_3, u_4), \quad u \in (u_1, u_2), \quad (25)$$

$$h(u; u_1, u_2) \geq h(u; u_3, u_4), \quad u \in (u_1, u_2). \quad (26)$$

Proof. The relation (24) is clear since $h(u) \leq f(u) \leq k(u)$. Let $(u_1, u_2) \subset (u_3, u_4)$. Then, since the sets given in (23) are ordered as $B(u_3, u_4) \subset B(u_1, u_2)$, the corresponding infimums should be ordered as in (25). Similarly we have (26). \square

We now consider properties of envelopes which are useful in the construction of signed N-waves. In the construction of an N-wave only the case with $\underline{u} = 0$ is used and hence we consider the case the following lemma.

Lemma 2. *1. If the convex envelope $h(u; 0, \bar{u}_0)$ is linear on $(a, b) \subset (0, \bar{u}_0)$, then $h(u; 0, \bar{u})$ is linear on (a, b) for all $\bar{u} \geq \bar{u}_0$. This property holds for the concave envelope, too.*

2. At least one of $h(u; 0, \bar{u})$ and $k(u; 0, \bar{u})$ is linear on $(\bar{u} - \varepsilon, \bar{u})$ for an $\varepsilon > 0$ small.

- Proof.** 1. Suppose that $h(u; 0, \bar{u})$ is not linear on (a, b) for some $\bar{u} \geq \bar{u}_0$. Then there exists a subinterval $(c, d) \subset (a, b)$ on which $h(u; 0, \bar{u})$ is strictly convex and hence $h(u; 0, \bar{u}) = f(u)$. Since $h(u; 0, \bar{u}_0)$ is linear on (c, d) and is a lower convex envelope of $f(u)$, $h(u; 0, \bar{u}_0) < f(u) = h(u; 0, \bar{u})$ on the interval (c, d) after taking a smaller interval if needed. It contradicts to Lemma 1 (26). Similar arguments hold for concave envelope $k(u; 0, \bar{u})$.
2. If $h(u; 0, \bar{u})$ is not locally linear near $u = \bar{u}$, then $h(u; 0, \bar{u}) = f(u)$ and strictly convex for $u \in (\bar{u} - \varepsilon, \bar{u})$. Therefore, the concave envelope can not be identical to $f(u)$ on the interval. Hence it should be linear on it. \square

4. N-waves for a general non-convex flux

4.1. Construction of N-waves

In this section we construct a positive N-wave $N_{0,q}(x, t)$ such that

$$N_{0,q}(x, t) \rightarrow q\delta(x) \quad \text{as } t \rightarrow 0$$

in a distribution sense, i.e., $N_{0,q}(x, t)$ is a delta sequence of weight $q > 0$ as $t \rightarrow 0$. A negative N-wave $N_{p,0}(x, t)$ can be similarly constructed. Even though the construction of an N-wave is a natural generalization of the convex flux case, there is a considerable complexity. In the followings we present it step by step comparing with the convex case and the figures in the later sections.

Due to the second hypothesis in (H1) there exists $\bar{u} > 0$ such that the jump discontinuity connecting $u_r = 0$ and $u_l = u$ is admissible for all $u \geq \bar{u}$. Therefore we may take $N_{0,q}(x, t) := \tilde{N}_{0,q}(x, t)$ until this moment. We do not need to know the maximal time period that the equality holds. We just want to find a moment $t_0 > 0$ and $b_q(t_0)$ such that

$$g(b_q(t_0)/t_0) = u_0 \geq \bar{u} \quad \text{and} \quad q = \int_0^{b_q(t_0)} g(y/t_0) dy, \quad (27)$$

where g is the rarefaction profile given by (19). Let

$$\bar{h}_0(u) = \inf\{x : N_{0,q}(x, t_0) > u\}, \quad \bar{k}_0(u) = \sup\{x : N_{0,q}(x, t_0) > u\}, \quad (28)$$

where \bar{k}_0 is constant in this setting. The union of graphs of \bar{h}_0 and \bar{k}_0 is simply the reflection of the graph of $\tilde{N}_{0,q}(x, t_0)$ with respect to the line $u = x$. In Figure 6 an example is given. In the first figure the graph of a flux f and corresponding $u_0 > 0$ are given. Clearly, the concave envelope $k(u; 0, u_0)$ is a straight line. The corresponding time t_0 and the graphs of \bar{h}_0 and \bar{k}_0 are given in the second one, where we took $q = 4$.

Consider the convex envelope $h(u; 0, u_0)$. Then there exists a maximal interval (v_0, u_0) such that $h(u; 0, u_0) = f(u)$ on it and v_0 is a tangent point.

Notice that the concave envelope $k(u; 0, \bar{u})$ changes a lot as \bar{u} moves from u_0 to v_0 . However, the convex envelope stays as it is (see Figure 6 for example). Therefore, for $v_0 < u < u_0$ and $t_0 < t$, we can define

$$\bar{h}(u, t) = \bar{h}_0(u) + \int_{t_0}^t h'(u; 0, u_0) d\tau, \quad v_0 \leq u \leq u_0, \quad (29)$$

where the derivative in the integrand is with respect to u of course. One can easily see that \bar{h} is an increasing function with respect to u variable. This function $\bar{h}(u, t)$ will give the increasing side of an N-wave.

The next step is to find the shock place $x = b_q(t)$ which corresponds to the one in (14). For the convex flux case the point has three important aspects that it is the right end point of the support, the place of a decreasing shock and the maximum point. For a general non-convex flux case it still is the maximum point, but it is not the end point of the support in general. Furthermore the N-wave may have an increasing shock at the corresponding point. Let $x = b_q(t)$ and $\bar{u}(t)$ is obtained by solving

$$b'_q(\tau) = \frac{f(\bar{u}(\tau)) - f(u_*(\tau))}{\bar{u}(\tau) - u_*(\tau)} \left(\equiv k'(u; 0, \bar{u}(\tau)) \text{ for } u_* \leq u \leq \bar{u}(\tau) \right), \quad (30)$$

$$b_q(\tau) = \bar{h}(\bar{u}(\tau), \tau), \quad (31)$$

where $u_*(\tau)$ is the end of the linear part of the concave envelope $k(u; 0, \bar{u}(\tau))$ that connects the other end $\bar{u}(\tau)$. Note that, if $\bar{u}(\tau)$ is given, u_* can be computed. For simple cases one can solve this system explicitly and an example is given in Section 4.2. However, it is not possible for a general case and that makes the N-wave remain implicit.

Now we show that $\bar{u}(t)$ decreases in time. Since the monotonicity is a local property, it is enough to consider $t_1 < t_2$ with $|t_1 - t_2| \ll 1$ small enough. By taking smaller $|t_1 - t_2|$ if needed we may assume, for all $t_1 < \tau, \tau' < t_2$,

$$k'(\bar{u}(\tau); 0, \bar{u}(\tau)) < h'(\bar{u}(t_1); 0, u_0).$$

due to the relation between the convex and the concave envelopes. Then we clearly have

$$b'_q(\tau) = k'(\bar{u}(\tau); 0, \bar{u}(\tau)) < h'(\bar{u}(t_1); 0, u_0) = \partial_t \bar{h}(\bar{u}(t_1), \tau),$$

Therefore, since $b_q(t_1) = \bar{h}(\bar{u}(t_1), t_1)$, we have

$$\bar{h}(\bar{u}(t_2), t_2) = b_q(t_2) < \bar{h}(\bar{u}(t_1), t_2).$$

Since $\bar{h}(\cdot, t)$ is an increasing function, we finally have

$$\bar{u}(t_2) < \bar{u}(t_1) \quad \text{for all } t_1 < t_2. \quad (32)$$

Now we may define the decreasing side of the N-wave

$$\bar{k}(u, t) = \bar{k}_0(u) + \int_{t_0}^t k'(u; 0, \bar{u}(\tau)) d\tau. \quad (33)$$

The concave envelope in the integrand depends on the maximum $\bar{u}(\tau)$ and, in other words, it counts the changes of the concave envelope which appears when the end point of the envelope moves from u_0 to v_0 . For $u \notin [0, \bar{u}(t)]$, we simply set $\bar{h}(u, t) = \bar{k}(u, t) := 0$.

One can easily check that, since $k'(u; 0, \bar{u}(\tau)) = \frac{f(\bar{u}(\tau)) - f(u_*(\tau))}{\bar{u}(\tau) - u_*(\tau)}$ for any fixed $v_0 < u < u_0$, $\bar{k}(u, t)$ actually moves with the same speed as $b_q(t)$ and hence

$$b_q(\tau) = \bar{k}(\bar{u}(\tau), \tau). \quad (34)$$

Therefore, $\bar{h}(\bar{u}(\tau), \tau) = \bar{k}(\bar{u}(\tau), \tau) = b_q(\tau)$ and hence we may define the N-wave using the inverse relation of these functions

$$\bar{h}(N_{0,q}(x, t), t) = x \text{ for } x < b_q(t), \quad \bar{k}(N_{0,q}(x, t), t) = x \text{ for } x > b_q(t). \quad (35)$$

In Figure 6 the graphs of \bar{h} and \bar{k} are displayed at $t = 0.085$ where $\bar{u}(t) = u_1$ is slightly bigger than v_0 . As $\bar{u}(t)$ approaches to v_0 the thin spike in the figure becomes thinner and eventually disappears and the maximum jumps from $\bar{u}(t) = v_0$ to $u_*(t)$ and the first stage of the N-wave is completed.

Now let v_1 be the tangent point of the concave envelope $k(u; 0, u_*)$. In the second stage the N-wave is constructed similarly in the interval $v_1 < u < u_*$. The difference is that the role of the convex and the concave envelopes are swapped. Since we have assumed that there is only finite number of inflection points, this process will be done in finite steps and the construction of the N-wave is completed.

Remark 5. One can clearly see that $\bar{u}(t)$ which was employed in the construction of the N-wave is the maximum of the N-wave, i.e.,

$$\bar{u}(t) \equiv \max_x N_{0,q}(x, t). \quad (36)$$

The monotonicity in (32) now implies that maximum of the N-wave decreases monotonically as $t \rightarrow \infty$.

Remark 6. For the convex case the inverse relation of the flux is considered first to find rarefaction profile g and then the time effect is counted simply by $g(x/t)$ as in (14). However, for the non-convex case, the convex-envelope varies as \bar{u} moves. Therefore, the time effect is considered first as in (29) and then the inverse relation (35) is considered, which is a more general way. For example, the convex case can be written similarly. Since $th'(g(x/t)) = x$, $g(x/t)$ is the inverse relation of the mapping $u \rightarrow th'(u) \equiv \int_0^t h'(u) d\tau$.

Now we discuss several basic properties of \bar{h} and \bar{k} in the followings. These immediately provide certain structures of fundamental solutions.

Lemma 3. 1. $\bar{h}(u, t)$ and $\bar{k}(u, t)$ are continuous for all $t \geq t_0$.

2. If the convex envelope $h(u; 0, \bar{u}(t))$ has a linear part that connects $u = a$ and $u = b$, then $\bar{h}(u, t)$ is constant for $u \in (a, b)$ and hence the corresponding N-wave $N_{0,q}(x, t)$ has an increasing shock that connects $u = a$ and $u = b$. Linear part of the concave envelope gives decreasing shock similarly.

3. The maximum point $(b_q(t), \bar{u}(t))$ of an N-wave is always connected to a shock one side and a rarefaction wave the other side.

Proof. 1. Since the envelopes are continuously differentiable, $\bar{h}(u, t)$ and $\bar{k}(u, t)$ are continuous.

2. Lemma 2 implies that $h'(u; 0, \bar{u}(\tau))$ is constant in $u \in (a, b)$ for any given time $0 < \tau < t$. Therefore, its integral with respect to time variable (29) is also constant on the interval. Clearly from the construction of $\bar{N}_{0,q}(x, t)$, $\bar{h}_0(u)$ is constant on the interval. Therefore, $\bar{h}(u, t)$ is constant on (a, b) and hence the inverse image $N_{0,q}(x, t)$ has the discontinuity in the claim. Similar arguments hold for concave envelopes.
3. If the maximum point is connected to shocks on both sides, that means it has a removable jump at the point. Lemma 2(2) implies that the maximum point cannot be connected by two rarefaction waves. Therefore, the maximum point is connected by an increasing shock and a decreasing rarefaction, or an increasing rarefaction and a decreasing shock. \square

Theorem 1. Let $N_{0,q}(x, t)$ be the positive N-wave given by the relation (35) and $N_{p,0}(x, t)$ be the corresponding negative N-wave under the hypothesis (H1). Then,

1. N-waves $N_{0,q}(x, t)$ and $N_{p,0}(x, t)$ are signed source type solutions of (1) with $M = q$ and $M = -p$, respectively.
2. Under the extra hypothesis (H2) the N-wave $N_{p,q}(x, t)$ given by (3) is a solution of (1) for all $p, q \geq 0$ such that $q - p = M$.

Proof. 1. We can easily check that the N-wave constructed here is really the admissible solution. Since the construction is done in a way that the Oleinik and the Rankine-Hugoniot conditions are satisfied, all we need to do is to show that the N-wave satisfies the equation in a classical sense in smooth regions. Assume that the N-wave is smooth at $x < b_q(t)$. First differentiate the first relation in (35) with respect to x and t and obtain

$$\frac{\partial}{\partial x} \left(\bar{h}(N_{0,q}(x, t), t) \right) = \left(\frac{\partial}{\partial u} \bar{h} \right) \left(\frac{\partial}{\partial x} N_{0,q} \right) = 1, \quad (37)$$

$$\frac{\partial}{\partial t} \left(\bar{h}(N_{0,q}(x, t), t) \right) = \left(\frac{\partial}{\partial u} \bar{h} \right) \left(\frac{\partial}{\partial t} N_{0,q} \right) + \frac{\partial}{\partial t} \bar{h} = 0. \quad (38)$$

On the rarefaction wave side the convex envelope and the flux itself are identical. Therefore, from (29),

$$\frac{\partial}{\partial t} \bar{h}(N_{0,q}(x, t), t) = h'(N_{0,q}(x, t); 0, \bar{u}(t)) = f'(N_{0,q}(x, t)). \quad (39)$$

Substituting (37) and (39) into (38), we finally obtain

$$\frac{\partial}{\partial t} N_{0,q}(x, t) + f'(N_{0,q}(x, t)) \frac{\partial}{\partial x} N_{0,q}(x, t) = 0.$$

On the region $x > b_q(t)$, one can similarly show equation by differentiating the second relation in (35), which completes the proof that $N_{0,q}(x, t)$ is a positive source type solution of the equation (1) with $M = q > 0$.

2. Since the flux f has the minimum value at origin, the smooth convex envelope has $h'(0) = 0$. Therefore, $h'(u) \geq 0$ for all $u \geq 0$ because of the convexity of h and hence $\bar{h}(u, t) \geq 0$ for all $t > 0$ and $u > 0$. Therefore the support of $N_{0,q}(x, t)$ for a fixed $t > 0$ belongs to $[0, \infty)$. Similarly one can show that the support of $N_{p,0}(x, t)$ for a fixed $t > 0$ belongs to $(-\infty, 0]$. Therefore, for all $t > 0$,

$$N_{p,q}(x, t) \Big|_{(-\infty, 0)} = N_{p,0}(x, t), \quad N_{p,q}(x, t) \Big|_{(0, \infty)} = N_{0,q}(x, t),$$

and hence all the shocks satisfy the Oleinik and Rankine-Hugoniot conditions and rarefaction waves satisfy the equation in a classical sense. Furthermore, $N_{p,q}(x, t)$ converges to $M\delta(x)$ as $t \rightarrow \infty$. \square

4.2. Examples and comparison with a convex case

In this section we consider examples that show the structure of the N-wave $N_{0,q}(x, t)$ constructed in the previous section. First consider the Burgers equation case in which case we already have N-waves and compare it with the N-waves in this paper. One may easily see that the construction of N-wave in this paper is a natural generalization of the well-known N-wave of the Burgers equation.

The flux of the Burgers equation is $f(u) = u^2/2$ which is convex. Therefore, the convex envelope is simply $h(u; 0, \bar{u}) = f(u)$ and the concave envelope is the linear line connecting the origin and $(\bar{u}, f(\bar{u}))$, i.e., $k(u; 0, \bar{u}) = \bar{u}u/2$. For the initial time we may take $t_0 = 1$. Then one can easily compute that $h'(u; 0, \bar{u}(t)) = u$, $k'(u; 0, \bar{u}(t)) = \bar{u}(t)/2$, $b_q(t_0) = \bar{u}(t_0) = \sqrt{2q}$ and hence the initial profiles in (28) are given by

$$\bar{h}_0(u) = u, \quad \bar{k}_0(u) = \sqrt{2q}.$$

Therefore,

$$\bar{h}(u, t) = u + \int_1^t u dt = tu, \quad \bar{k}(u, t) = \sqrt{2q} + \int_1^t \bar{u}(t)/2 dt.$$

Now we solve $b_q(t)$ and $\bar{u}(t)$ in (30)-(31). Since

$$b_q(t_0 = 1) = \sqrt{2q}, \quad b_q(t) = \bar{h}(\bar{u}(t), t) = t\bar{u}(t), \quad \frac{f(\bar{u}(t))}{\bar{u}(t)} = \bar{u}(t)/2,$$

the equation (30) becomes

$$b'_q(t) = b_q(t)/2t, \quad b_q(1) = \sqrt{2q}.$$

One can easily compute this first order equation and obtain

$$b_q(t) = \sqrt{2qt}, \quad \bar{u}(t) = \sqrt{2q/t},$$

which gives the same N-wave in (11) after taking inverse relation in (35).

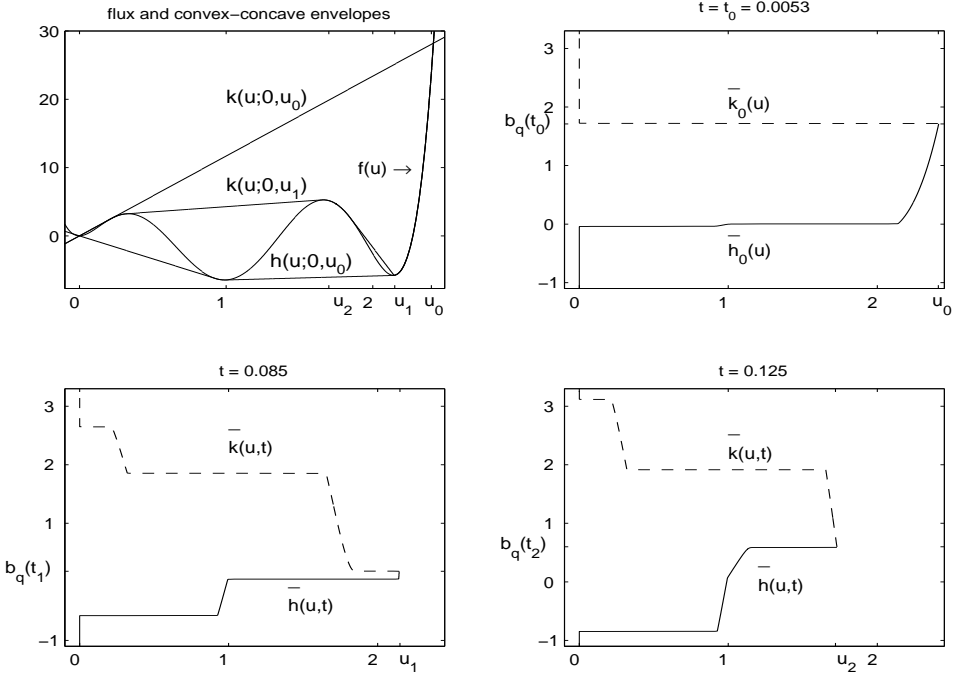


Fig. 6. The flux and the envelopes are given for two cases, $k_i := k(u; 0, u_i)$, $h_i := h(u; 0, u_i)$, $i = 0, 1$. u_0 is the value that shock that connects $u_l = u_0$ and $u_r = 0$ is admissible. This gives the initial profile $\bar{h}_0(u)$ and $\bar{k}_0(u)$. As $\bar{u}(t)$ decreases or as the time t increases, $\bar{h}(u, t)$ and $\bar{k}(u, t)$ may show interesting behavior.

For a general non-convex flux case it is not possible to solve the equations by hands and one needs to compute it numerically using appropriate iterative method. However, the properties given in Lemmas 2 and 3 enable us to see the structure of the N-wave via the structures of $\bar{h}(u, t)$ and $\bar{k}(u, t)$.

In Figure 6 several examples are given. In the first figure the graph of the flux and convex-concave envelopes are shown. This flux satisfies the hypothesis (H1) only. Since the convex envelope has a linear part with negative slope, the corresponding shock has negative speed. The concave envelope $k(u; 0, u_0)$ is a straight line. One can find in the figure at $t = 0.0053$ that $\bar{k}_0(u)$ is constant. The convex envelope $h(u; 0, u_0)$ consists of two linear parts and two nonlinear parts. In the graph of $\bar{h}_0(u)$ one can find two constant parts and two rarefaction parts.

The concave envelope $k(u; 0, u_1)$ consists of three straight lines and two nonlinear curves. One can find from the figure at $t = 0.085$ that $\bar{k}(u, t)$ has three constant parts and two rarefaction waves. Note that in this example we took $q = 4$. The convex envelope $h(u; 0, u_1)$ consists of two linear parts and one nonlinear part. In the graph of $\bar{h}_0(u)$ one can find two constant states

and one rarefaction wave. However, at the end there is a short increasing rarefaction wave. That means that u_1 is slightly bigger than the tangent point of the convex envelope.

If u_1 arrives at the tangent point, then the thin pick will be disappeared and there will be a jump in the maximum point $\bar{u}(t)$. This spike is gone in the figure at $t = 0.125$. One interesting point is the angle in the middle of the rarefaction wave of $\bar{h}(u, t)$ in the last picture. This is due to the sudden change of the convex envelope that happened when the spike was collapsed. Finally, the corresponding N-wave is obtained from the relations in (35), i.e., the N-wave $N_{0,4}(x, t)$ is obtained by simply reflecting the figures with respect to the line $y = x$. As we have observed from these examples the structure of the envelopes indicates the shape of an N-wave.

5. Numerical examples

In this section we compare N-waves constructed in the previous section and numerical simulations for the N-wave. In the computation we employed the WENO and a central type scheme (see [5, 8, 17]). These tests show that the numerical solutions exactly show the structure of the N-wave discussed previous section. For the test we consider non-convex fluxes given by

$$f_n(u) = u^n(u^2 - 2u + 1.02)(u^2 - 4u + 4.02), \quad n \geq 2, \quad (40)$$

which satisfies both of the hypotheses (H1) and (H2). For the numerical computation one should consider appropriate initial value. It is clear that the dirac-delta measure can not be used directly. We take an initial value given by

$$u_t + f_n(u)_x = 0, \quad (41)$$

$$u_0(x) = \begin{cases} q/\epsilon, & 0 < x < \epsilon, \\ 0, & \text{otherwise,} \end{cases} \quad (42)$$

where q/ϵ is large enough that the jump from $u_l = q/\epsilon$ to $u_r = 0$ is admissible. Then $u(x, t) = N_{0,q}(x, t)$ for $t > 0$ such that $\max u(x, t) < q/\epsilon$.

In Figure 7 intermediate states of the N-wave $N_{0,1}(x, t)$ are given at three instances. The first one at $t = 0.14$ has the maximum value corresponding to u_1 in Figure 5(a). The concave envelope at the moment consists of two linear parts and one rarefaction part. Since the amount of time to form a rarefaction is very short, one can barely find a rarefaction wave in the figure. One can find the corresponding rarefaction wave more clearly in the graph at $t = 1$. The concave envelope at the moment with the maximum u_2 in the Figure 5(a) has three linear parts and two rarefaction waves and one can find them in the decreasing profile of the N-wave. At $t = 4$ the corresponding maximum is u_3 and the concave envelope has two linear part and one rarefaction wave. In the Figure at $t = 4$ one can observe two shocks and one rarefaction. One can also find a cusp in the rarefaction wave. That is formed due to the sudden change of concave envelope from k_2 to k_3 .

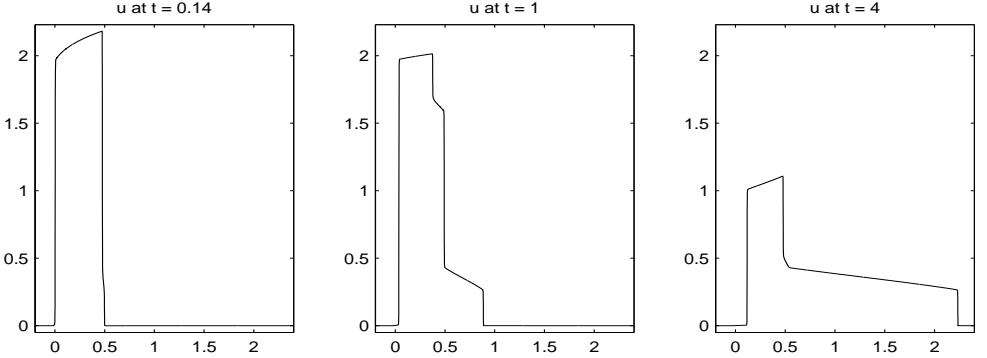


Fig. 7. Numerical computations of N-wave $N_{0,1}(x, t)$ are given at three instances. The flux f_2 in (40) is considered. For this numerical computation we used WENO scheme and the central scheme also gives similar results.

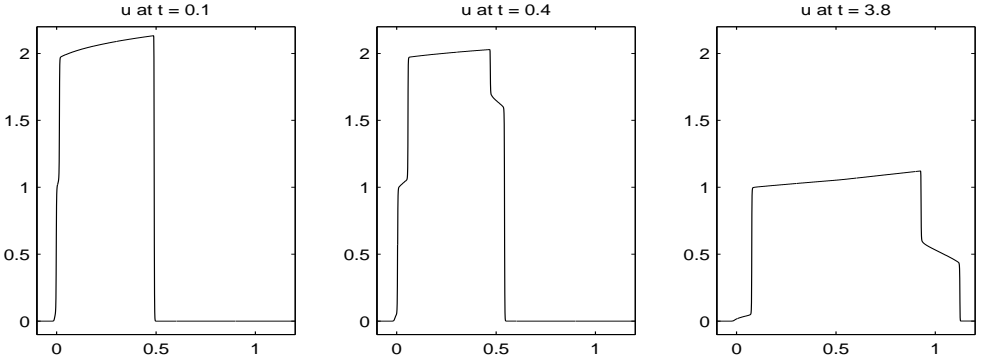


Fig. 8. Numerical computations of N-wave $N_{0,1}(x, t)$ are given at three instances. The flux f_n in (40) with $n = 3$ is considered. For this numerical computation we used WENO scheme and the central scheme also gives similar results.

In Figure 8 another example for intermediate states of an N-wave are given with the flux function f_n with $n = 3$. The figures of its graph and concave envelopes are also given in Figure 5(b). From these figures one can see that this numerical examples have the structure discussed Section 4.

Now we consider the asymptotic structure of the N-wave. Notice that, even if the formulas in (29) and (33) enable us to view the structure of the N-wave in detail, it is not easy to compute it exactly. That is why we could not display the examples in Figures 7 and 8 with exact solutions. However, for the asymptotic structure, one can easily compute the N-wave exactly since the structure of the N-wave depends on the structure of the flux near $u = 0$. For example, under the hypothesis (H2), if the maximum of the N-wave is less than the smallest tangent value of the convex envelope, then $N_{0,q}(x, t) = \tilde{N}_{0,q}(x, t)$ and hence one can easily compute the N-wave.

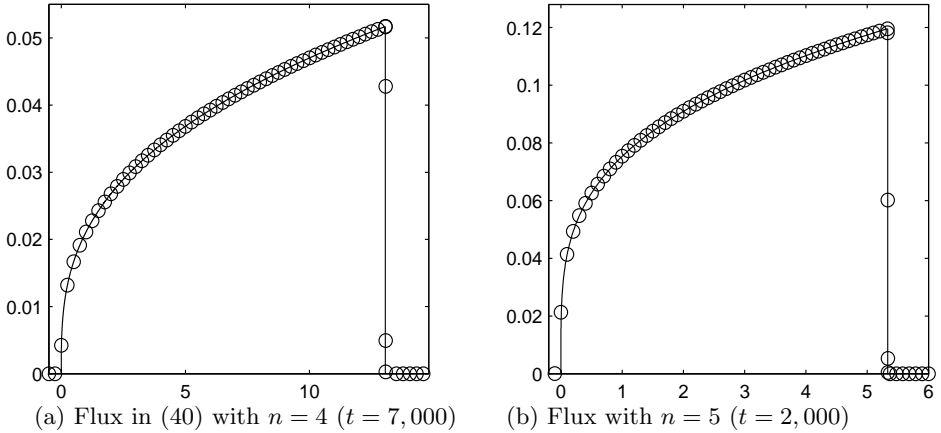


Fig. 9. The exact N-waves $N_{0,0.5}(x, t)$ are given in solid line together with a numerical solution. They match well. A central type scheme is used for the numerical solution.

In Figure 9(a) the exact N-wave $N_{0,0.5}(x, t)$ is given in a solid line together with a numerical solution, where the flux is f_n with $n = 4$. For an easier comparison with the exact solution the numerical solution is plotted using less grid points. One can clearly see that the numerical solution matches to the N-wave. For this numerical example we used the central scheme. The example with f_n with $n = 5$, Figure 9(b) also matches to the exact N-wave well.

References

1. D.P. Ballou, *Solutions to nonlinear hyperbolic Cauchy problems without convexity conditions*. Trans. Amer. Math. Soc. **152** (1970), 441–460.
2. J.A. Carrillo and J.L. Vazquez, *Fine asymptotics for fast diffusion equations*. Comm. Partial Differential Equations **28** (2003), 1023–1056.
3. C.M. Dafermos, *Generalized characteristics and the structure of solutions of hyperbolic conservation laws*. Indiana Univ. Math. J., **26** (1977), 1097–1119.
4. C.M. Dafermos, *Regularity and large time behaviour of solutions of a conservation law without convexity*. Proc. Roy. Soc. Edinburgh Sect. A **99** (1985), 201–239.
5. Y. Ha and Y.-J. Kim, *Explicit solutions to a convection-reaction equation and defects of numerical schemes*. J. Comput. Phys. **220** (2006), 511–531.
6. D. Hoff, *The sharp form of Oleinik's entropy condition in several space variables*. Trans. Amer. Math. Soc. **276** (1983), 707–714.
7. H.K. Jenssen and C. Sinestrari, *On the spreading of characteristics for non-convex conservation laws*. Proc. Roy. Soc. Edinburgh Sect. A **131** (2001), 909–925.
8. G.-S. Jiang and C.-W. Shu, *Efficient Implementation of Weighted ENO schemes*. J. Comput. Phys. **126** (1996), 271–292.
9. Y.-J. Kim, *Piecewise Self-similar Solutions and a Numerical Scheme for Scalar Conservation Laws*. SIAM J. Numer. Anal. **40** (2002), 2105–2132.

10. Y.-J. Kim, *Asymptotic behavior of solutions to scalar conservation laws and optimal convergence orders to N -waves*. J. Differential Equations **192** (2003), 202–224.
11. Y.-J. Kim and Y.-R. Lee, *Structure of fundamental solutions of a conservation law without convexity*. <http://amath.kaist.ac.kr/~ykim/preprints/17.pdf>
12. Y.-J. Kim and R. McCann, *Potential theory and optimal convergence rates in fast nonlinear diffusion*. J. Math. Pures Appl. **86** (2006), 42–67.
13. S. N. Krushkov, *First-order quasilinear equations with several space variables*. Mat. Sb., **123** (1970), 228–255.
14. P.D. Lax, *Hyperbolic systems of conservation laws. II*. Comm. Pure Appl. Math., **10** (1957), 537–566.
15. T.-P. Liu and M. Pierre, *Source-solutions and asymptotic behavior in conservation laws*. J. Differential Equations **51** (1984), 419–441.
16. T.G. Myers, *Thin films with high surface tension*. SIAM REV. **40** (1998) 441–462.
17. H. Nessyahu and E. Tadmor, *Nonoscillatory central differencing for hyperbolic conservation laws*. J. Comput. Phys. **87** (1990), 408–463.
18. O.A. Oleinik, *Discontinuous solutions of non-linear differential equations*. Amer. Math. Soc. Transl. **26** (1963), 95–172.
19. T. Tang, Z.-H. Teng and Z. Xin, *Fractional rate of convergence for viscous approximation to nonconvex conservation laws*. SIAM J. Math. Anal. **35** (2003), 98–122.
20. B. Wendroff, *The Riemann problem for materials with nonconvex equations of state. I. Isentropic flow*. J. Math. Anal. Appl. **38** (1972), 454–466.
21. B. Wendroff, *The Riemann problem for materials with nonconvex equations of state. II. General flow*. J. Math. Anal. Appl. **38** (1972), 640–658.

Yong-Jung Kim

Department of Mathematical Sciences, KAIST
335 Gwahangno, Yuseong-gu, Daejeon 305-701, Republic of Korea
email:yongkim@kaist.edu

and

Youngsoo Ha

Department of Mathematical Sciences, KAIST
335 Gwahangno, Yuseong-gu, Daejeon 305-701, Republic of Korea
email:youngsoo@amath.kaist.ac.kr